Toward deterministic construction of low noise avalanche photodetector materials

A. K. Rockwell, M. Ren, M. Woodson, A. H. Jones, S. D. March, Y. Tan, Y. Yuan, Y. Sun, R. Hool, S. J. Maddox, M. L. Lee, A. W. Ghosh, J. C. Campbell, and S. R. Bank

Citation: Appl. Phys. Lett. **113**, 102106 (2018); doi: 10.1063/1.5040592

View online: https://doi.org/10.1063/1.5040592

View Table of Contents: http://aip.scitation.org/toc/apl/113/10

Published by the American Institute of Physics

Toward deterministic construction of low noise avalanche photodetector materials

A. K. Rockwell,[1,a)] M. Ren,[2] M. Woodson,[2] A. H. Jones,[2] S. D. March,[1] Y. Tan,[2] Y. Yuan,[2] Y. Sun,[3] R. Hool,[4] S. J. Maddox,[1] M. L. Lee,[3] A. W. Ghosh,[2,5] J. C. Campbell,[2] and S. R. Bank[1,a)]

[1]*Department of Electrical and Computer Engineering, University of Texas, Austin, Texas 78758, USA*
[2]*Department of Electrical and Computer Engineering, University of Virginia, Charlottesville, Virginia 22904, USA*
[3]*Department of Electrical and Computer Engineering, University of Illinois, Urbana, Illinois 61801, USA*
[4]*Department of Materials Science and Engineering, University of Illinois, Urbana, Illinois 61801, USA*
[5]*Department of Physics, University of Virginia, Charlottesville, Virginia 22904, USA*

(Received 18 May 2018; accepted 20 August 2018; published online 7 September 2018)

Over the past 40+ years, III-V materials have been intensively studied for avalanche photodetectors, driven by applications including optical communications, imaging, quantum information processing, and autonomous vehicle navigation. Unfortunately, impact ionization is a stochastic process that introduces noise, thereby limiting sensitivity and achievable bandwidths, leading to intense effort to mitigate this noise through the identification of different materials and device structures. Exploration of these materials has seen limited success as it has proceeded in a largely *ad hoc* fashion due to little consensus regarding which fundamental properties are important. Here, we report an exciting step toward deterministic design of low-noise avalanche photodetector materials by alternating the composition at the monolayer scale; this represents a dramatic departure from previous approaches, which have concentrated on either unconventional compounds/alloys or nanoscale band-engineering. In particular, we demonstrate how to substantially improve upon the noise characteristics of the current state-of-the art telecom avalanche multipliers, $In_{0.52}Al_{0.48}As$ grown on InP substrates, by growing the structure as a strain-balanced digital alloy of InAs and AlAs layers, each only a few atomic layers thick. The effective *k*-factor, which has historically been considered a fundamental material property, was reduced by 6–7× from $k = 0.2$ for bulk $In_{0.52}Al_{0.48}As$ to $k = 0.05$ by using the digital alloy technique. We also demonstrate that these "digital alloys" can significantly extend the photodetector cutoff wavelength well beyond those of their random alloy counterparts. *Published by AIP Publishing.* https://doi.org/10.1063/1.5040592

Avalanche photodiodes (APDs)[1] have been utilized for a wide range of commercial, military, and research applications.[2–6] The primary advantage of APDs relative to other photodetectors is their internal gain originating from impact ionization, which can provide higher sensitivity. However, gain is concomitant with noise. For the APDs, this noise arises from the stochastic nature of impact ionization. Photogenerated carriers injected into the high-electric-field multiplication region initiate a series of sequential ionization events, the number of which dictates the gain. Since impact ionization is not deterministic, there is a distribution of gain values. These gain fluctuations are a source of noise that is characterized by a figure of merit referred to as the excess noise factor, F(M).[7–9] The mean-squared shot-noise current can be expressed as[7]

$$\langle i_{shot}^2 \rangle = 2q(I_{ph} + I_{dark})M^2F(M)\Delta f, \tag{1}$$

where I_{ph} and I_{dark} are the primary photocurrent and dark current, respectively, M is the average avalanche gain, and Δf is the bandwidth. In the local field model,[7] the excess noise factor is given by

$$F(M) = kM + (1-k)(2 - 1/M), \tag{2}$$

where $k = \alpha/\beta$, the ratio of the electron, α, and hole, β, ionization coefficients for the case of pure electron injection. The excess noise factor increases with increasing gain but increases more slowly for lower values of *k*. It follows that higher receiver sensitivities are achieved with lower *k* values. Much of the research on improving materials and structures for APDs has been directed at reducing the excess noise factor. One approach has been to identify materials with advantageous impact ionization characteristics such as Si,[10–13] $Hg_{0.7}Cd_{0.3}Te$,[14,15] or InAs.[16–20] While these materials have excellent noise characteristics, there are wide spectral regimes that are not covered, and HgCdTe and InAs exhibit high dark current at room temperature due to their small bandgaps. Another approach to achieving low noise is introducing appropriately designed quantum wells and/or heterojunctions,[21,22] an approach known as impact ionization engineering (I^2E) with appropriately designed heterostructures.[23–31] This approach relies on the differences in threshold energies for impact ionization between adjacent wide-bandgap and narrow-bandgap materials. Initial work that demonstrated the efficacy of this approach used the GaAs/$Al_xGa_{1-x}As$ material system.[24–29] Previously, low excess noise has been achieved by designing thinner multiplication

a)Authors to whom correspondence should be addressed: akrockwell@utexas.edu and sbank@utexas.edu

regions to take advantage of non-local effects and using random alloy (RA) InAlAs multiplication layers.[32,33] Using this approach, Nada *et al.* have reported InAlAs/InGaAs APDs, for which the k value was limited to ~0.2.[34] While this has been an improvement on current technology, there needs to be a significant improvement in k to compete with Si and Ge/Si APDs. Duan *et al.* utilized the I^2E approach in an MBE-grown InGaAlAs I^2E separate absorption, charge, and multiplication (SACM) APD[31] and reported an excess noise equivalent to a k value of ~0.12. An enhancement of this approach is to cascade multiple I^2E multiplication cells, all operated at relatively low gain.[35–37] Proper design of the connection between two adjacent multiplication cells can significantly enhance impact ionization of the carrier type with a higher ionization rate and suppress impact ionization of the carrier with a lower ionization rate.[38] Ferraro *et al.* have reported a three-stage tandem I^2E APD with the InAlAs/InGaAlAs impact-ionization-engineered multiplication region which achieved $k = 0.05$ at $M = 10$ and $k = 0.1$ at $M = 20$.[39] While these structures have achieved low excess noise, their epitaxial layer structure is very complex, e.g., the structure in Ref. 39 consisted of 21 epitaxial layers, 15 of which required very precise control of doping and thickness. Recently, our group achieved very low noise, $k \sim 0.01$–0.05, with the $Al_xIn_{1-x}As_ySb_{1-y}$ ($x = 0.7$, 0.6, and 0.5) APD grown lattice matched to GaSb by MBE as digital alloys (DAs).[40,41] The fact that $Al_xIn_{1-x}As_ySb_{1-y}$ is a direct bandgap material under 76% Al means that it could also achieve higher speed operation than indirect bandgap materials in the mid- to near-infrared. A question regarding these APDs is whether $Al_xIn_{1-x}As_ySb_{1-y}$ is inherently a low-noise material such as Si, HgCdTe, and InAs or the result of digital alloy growth. Unfortunately, random alloys of the $Al_xIn_{1-x}As_ySb_{1-y}$ phase segregate, so it is difficult to compare random and digital alloys of this material. In this paper, we compare the random alloy $In_{0.52}Al_{0.48}As$ (referred to in the following as InAlAs) and $In_{0.53}Ga_{0.47}As$ (referred to in the following as InGaAs) lattice-matched to InP, both of which have been widely used as the multiplication region in high-performance telecommunication[1,32,34,42] APDs, with InAlAs and InGaAs grown as strain-balanced digital alloys of InAs/AlAs and InAs/GaAs, respectively. We demonstrate that the digital alloy growth significantly improves the noise characteristics of only InAlAs, relative to the random alloy, and extends the cutoff wavelength in both material systems. This work demonstrates the potential to reduce the noise and extend the operating wavelength, likely leading to an improvement of the gain-bandwidth product, of existing materials via the digital alloy growth method. Supporting experiments seek to clarify the origin of the noise enhancement.

Recent advances in crystal growth techniques have enabled device tailoring on the atomic scale. Specifically, the increased understanding of surfactant mediated growth, the effect of growth temperature, and the ability to control material deposition on the sub-monolayer scale have allowed for high-quality digital alloy growth.[43–45] These advances suggest the potential for deterministically designing APD materials on the few atom scale, the results of which will be discussed later in this paper.

Samples were grown by molecular beam epitaxy on n-type (100) InP substrates. The substrate temperature was held at 420 °C as determined using a pyrometer (k-Space BandiT), the In, Ga, and Al fluxes were adjusted so that the growth rate of each binary on InP and GaAs was 0.7 ML/s, and the As valve was adjusted so that the As_2/In beam-equivalent pressure (BEP) ratio was 5 and the flux ratio was 1.1. For the digital alloy period, we chose a nominal thickness of 6–10 monolayers (ML) or 1.7–2.9 nm, which was a compromise between being sufficiently thin that the electron and hole wave functions would overlap multiple periods and sufficiently thick that shutter transient effects would be adequately small. Coherent growth and well-defined superlattice fringes were evident in X-ray diffraction (XRD) reciprocal space mapping. The smooth and well-defined interfaces observed by transmission electron microscopy (TEM) shown in Fig. 1(a) suggest excellent control over the digital alloy growth, with no visible defects over the imaged area. A representative TEM scan for InAlAs digital alloys is shown in Fig. 1(b). Atomic force microscopy (AFM) studies confirmed the excellent material morphology, with a low root mean squared (RMS) roughness of ~0.25 nm over a scan area of 2 μm^2.

Avalanche photodiodes with 200 nm digital alloy p-type regions and 600 nm digital alloy multiplication regions, thick enough to avoid dead space effects,[46] were fabricated into circular mesas with standard photolithography and chemically

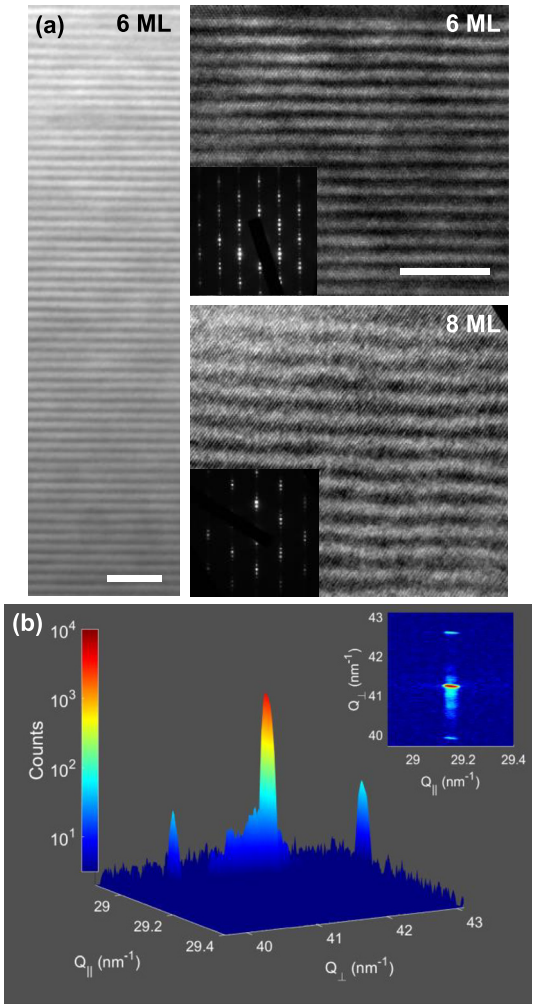

FIG. 1. (a) Bright-field TEM image under g = (002) (left) and g = (220) (right) two-beam conditions shows no evidence of extended defects in either a 6 monolayer (ML) or 8 ML InAlAs digital alloy. The scale bar is 10 nm. (b) (224) reciprocal space map for a 300 nm-thick 8 ML period InAlAs digital alloy. The inset shows the 2D intensity map.

etched with H_3PO_4:H_2O_2:H_2O (1:1:10). A window region in the top InGaAs layer was formed using an AZ 300 MIF photoresist developer. As shown previously,[40] sidewall passivation was achieved using a common photoresist, SU-8. Finally, titanium/gold contacts were deposited using e-beam evaporation. Excess noise measurements, shown in Figs. 2(a)–2(c), were extracted from photocurrent measured with an HP 8970 noise figure meter and a 543-nm He-Ne CW laser. The solid lines correspond to k-values from 0 to 0.5 using the local-field model.[7] The measured excess noise of the InGaAs [Fig. 2(a)] and AlGaAs [Fig. 2(b)] digital alloy APDs did not differ significantly from their random alloy counterparts.[47,48] However, we observed a significant decrease in excess noise in the InAlAs [Fig. 2(c)] digital alloy compared with both accepted literature and experimental values of $k \sim 0.2$. The InAlAs digital alloys in this work exhibit a k value of ~0.03, nearly as low as state-of-the-art Si APDs.[10–13] As the APDs shown below all had relatively thick multiplication regions (600 nm), we believe that the measured k-values are representative of the bulk ionization properties of 6 and 8 monolayer period InAlAs digital alloys.

Several possible effects could explain the observed noise reduction. First, digital alloys could be viewed as simply a highly scaled version of the MQW APDs where the impact ionization threshold is modulated with the composition.[21,22] This is similar to Capasso's staircase APD[49,50] in which an electron can gain a large amount of energy when moving from a large bandgap material to a small bandgap material, allowing for deterministic impact ionization. This view would suggest that key parameters would be (1) a large conduction band offset, relative to the bandgap, to enhance electron-related impact ionization and potentially (2) an indirect-direct bandgap transition between the constituent materials to enhance scattering and initiate impact ionization. The need for both of these factors in designing a low-noise APD could explain why both InGaAs [Fig. 2(d)] and AlGaAs [Fig. 2(e)] digital alloy based APDs do not show significantly lower excess noise, while InAlAs [Fig. 2(f)] digital alloy based APDs do.

A second explanation could be that superlattice band effects[51] might disproportionately suppress β because of narrower minibands with a higher radius of curvature dispersion due to the comparatively larger effective mass. This would suggest that larger valence band offsets and larger hole masses would be beneficial in material selection. This is consistent with the noise results of InGaAs and InAlAs digital alloys shown in Fig. 2; however, as shown in Figs. 3(a) and 3(b), the digital alloy band structure for both electrons and holes, calculated with tight-binding, is significantly distorted in the case of InAlAs but not in InGaAs, making it difficult to draw firm conclusions. Insights into α and β can be drawn by fitting[52]

$$M = \left\{1 - \int_0^W \alpha \exp\left[-\int_0^x (\alpha - \beta)dx'\right]dx\right\}^{-1}, \qquad (3)$$

where $k = \beta/\alpha = 0.03$ for the digital alloys and $k = 0.21$ for the random alloys, obtained from excess noise measurements. These fits support the role of modified valence band transport, given the significant suppression of β and only modest suppression of α as seen in Fig. 3(c), consistent with band structure calculations.

To further examine the second hypothesis, two 70% Al quaternary AlInAsSb digital alloy APDs were grown on GaSb in the manner of Ref. 53. One was nominally identical to that reported in Ref. 40, while the other was modified by combining the AlSb/AlAs/AlSb portion of the digital alloy into a single ternary layer of $AlAs_{0.10}Sb_{0.90}$, with an identical average composition. Comparing the band diagrams in Figs.

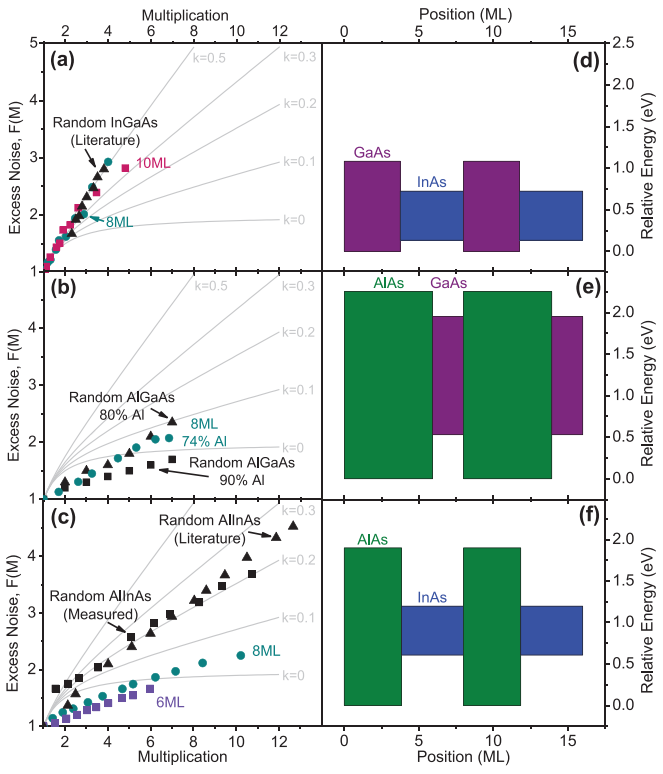

FIG. 2. (a) Excess noise factor vs. multiplication for both random and digital alloys of InGaAs[47] and (b) AlGaAs showing no difference in excess noise factors. (c) Excess noise factor vs. multiplication of InAlAs[48] alloys, exhibiting a significant decrease in the excess noise factor for digital alloys compared with random alloys from both the experiment and the literature. Band alignments for 2 periods of an (d) InGaAs digital alloy, (e) an AlGaAs digital alloy, and (f) an InAlAs digital alloy, accounting for strain, are shown.[52]

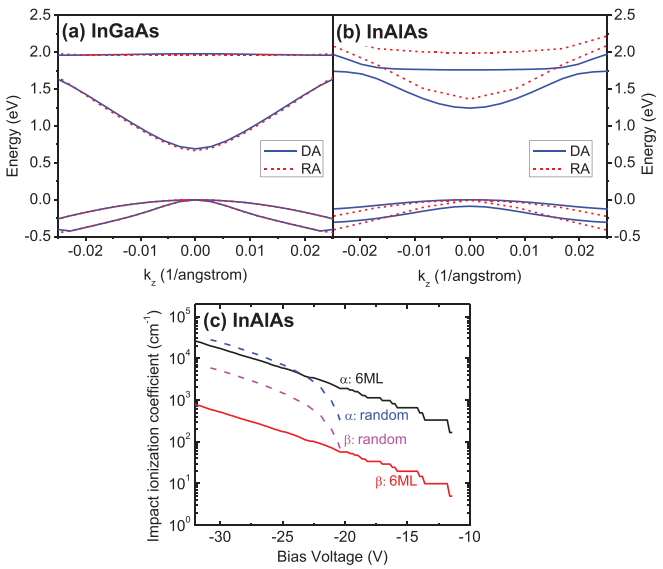

FIG. 3. Difference between random (RA) and digital alloy (DA) band structures of (a) InGaAs and (b) InAlAs, calculated with tight-binding. (c) Electron and hole impact ionization coefficients for InAlAs digital and random alloys, extracted from gain curves, suggesting that the suppression of hole impact ionization causes the reduction in excess noise.

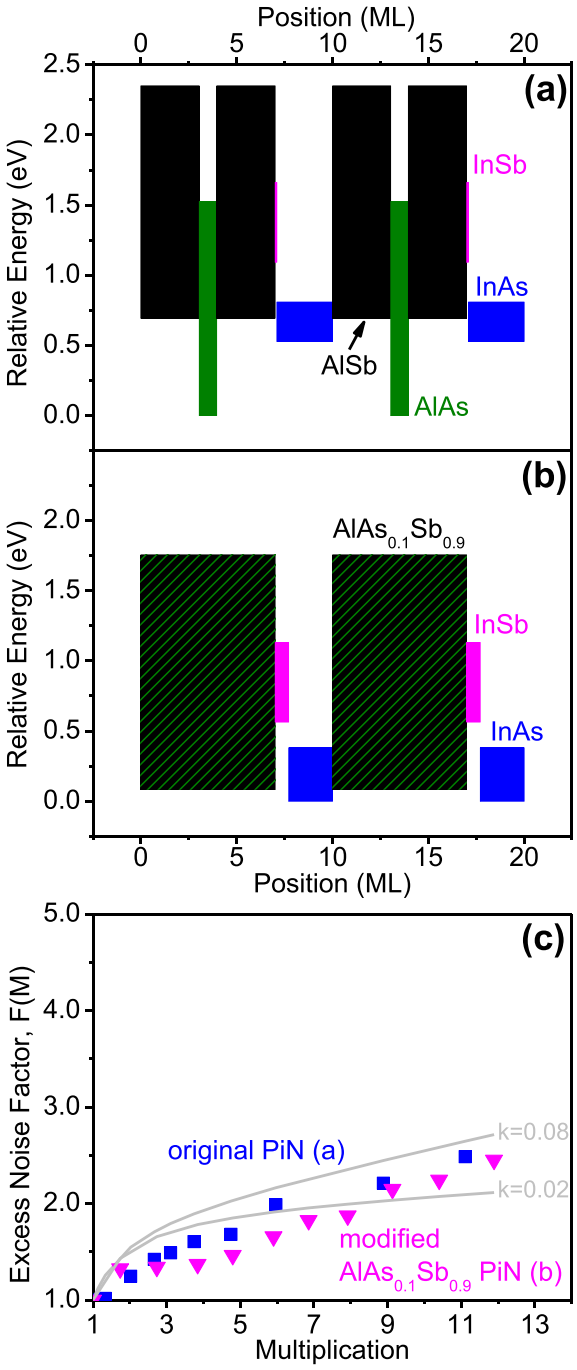

FIG. 4. Band alignments for 2 periods of the (a) original 70% Al quaternary AlInAsSb digital alloy and (b) modified $AlAs_{0.1}Sb_{0.9}$ 70% Al quaternary AlInAsSb digital alloy. (c) Excess noise factor vs. multiplication for both the original (blue symbols) and modified (pink symbols) 70% Al quaternary AlInAsSb APDs, showing no discernable difference.

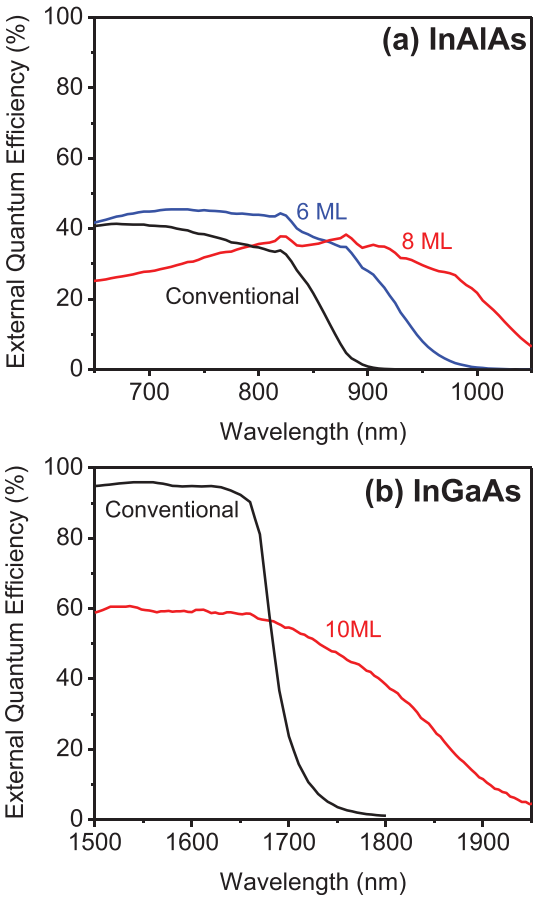

FIG. 5. (a) InAlAs and (b) InGaAs digital alloys exhibiting cutoff wavelength extension with the increasing period thickness.

4(a) and 4(b), it is found that this modification eliminates the largest portion of the valence band offset due to the asymmetric bowing between the conduction band and valence band edges in this alloy, which should greatly reduce miniband formation and modification to the hole transport.[54]

Since low-noise, with $k < 0.08$, was observed for both compositions [Fig. 4(c)], this suggests that valence band engineering may not be the dominant source of noise reduction in digital alloy APDs. We note, however, that modulation of the effective mass between binary layers can also induce miniband formation, even without a band discontinuity between the layers. This effect is shown in the supplementary material, along with a summary table of effective k-values, using the Kronig-Penney model,[55] and future studies will examine whether it is sufficient to explain the reduction in β observed in Fig. 3(c).

The digital alloy growth method also enables extension of the cutoff wavelength, as compared to their random alloy analogs. As shown in Fig. 5, the cutoff wavelength increased with the increasing period thickness, for both InGaAs and InAlAs, consistent with the effective bandgap calculated for InAlAs and InGaAs digital alloys shown in the supplementary material. This is particularly useful in the case of InGaAs as it allows for wavelength tuning of devices by simply adjusting the period thickness, whereas traditional approaches to extending the cutoff wavelength require metamorphic growth, resulting in extended defects that severely degrade the device dark current. By digital alloying the InAlAs material system, the cutoff wavelength was extended from approximately 900 nm to 1100 nm with an 8 ML period digital alloy [Fig. 5(a)]. Similarly, the InGaAs cutoff wavelength increased from ~1700 nm to greater than 1900 nm with a 10 ML period [Fig. 5(b)]. It is likely that the InGaAs cutoff wavelength can be extended further into the near-infrared by increasing the period thickness via surfactant-mediated growth. The external quantum efficiencies of the digital alloys in Figs. 5(a) and 5(b) can be enhanced through increased absorber layer thickness and the application of antireflection coatings. The "conventional" trace in Fig. 5(b)

is a commercial detector which has been optimized, leading to higher external quantum efficiency (EQE).

Despite significant research, short period superlattice detectors have not proven to be significantly more sensitive than their random alloy counterparts due to the requirements necessary to produce low noise in these devices. Here, we have demonstrated that by digitally alloying InAlAs, a workhorse of fiber telecom APDs, we can improve the impact ionization characteristics well beyond the state-of-the-art (k-factor reduced by 6–7×), which has historically been considered a fundamental material property. The large reduction in the k-factor will lead to higher sensitivities and achievable bandwidths. Combining InGaAs digital alloy absorbers with InAlAs digital alloy multipliers has the potential to achieve longer cutoff wavelengths and greater receiver sensitivities than are currently achievable on InP. More broadly, the digital alloying technique promises an innovative alternative to traditional APDs designed for detection across the visible and near-infrared wavelengths.

See supplementary material for a representative atomic force microscopy image of InAlAs digital alloys, along with various InAlAs APD device parameters, all showing the consistent and reproducible device quality we can achieve. It also includes calculated band structures of InAlAs and InGaAs digital alloys and Kronig-Penny calculations showing the emergence of bandgaps with mismatched effective masses.

This work was supported by the Army Research Office (W911NF-17-1-0065) and DARPA (GG11972.153060), as well as a University of Texas Temple Foundation Fellowship.

[1]J. C. Campbell, J. Lightwave Technol. **34**, 278 (2016).
[2]A. Tosi, N. Calandri, M. Sanzaro, and F. Acerbi, IEEE J. Sel. Top. Quantum Electron. **20**, 3803406 (2014).
[3]J. C. Campbell, *Optical Fiber Telecommunications VA: Components and Subsystems*, edited by I. Kaminow, T. Li, and A. E. Wilner (Academic Press, 2008), p. 221.
[4]N. Bertone and W. R. Clark, Laser Focus World **43**, 69 (2007), www.laserfocusworld.com/articles/print/volume-43/issue-9/features/apd-arrays-avalanche-photodiode-arrays-provide-versatility-in-ultrasensitive-applications.html.
[5]P. Mitra, J. D. Beck, M. R. Skokan, J. E. Robinson, J. Antoszewski, K. J. Winchester, A. J. Keating, T. Nguyen, K. K. M. B. D. Silva, C. A. Musca *et al.*, Proc. SPIE **6232**, 62320G (2006).
[6]G. M. Williams, Jr., Opt. Eng. **56**, 031224 (2017).
[7]R. C. J. McIntyre, IEEE Trans. Electron Devices **13**, 164 (1966).
[8]N. Z. Hakim, B. E. A. Saleh, and M. C. Teich, IEEE Trans. Electron Devices **37**, 599 (1990).
[9]M. Teich, K. Matsuo, and B. Saleh, IEEE J. Quantum Electron. **22**, 1184 (1986).
[10]C. A. Lee, R. A. Logan, R. L. Batdorf, J. J. Kleimack, and W. Wiegmann, Phys. Rev. **134**, A761 (1964).
[11]J. Conradi, IEEE Trans. Electron Devices **19**, 713 (1972).
[12]W. N. Grant, Solid-State Electron. **16**, 1189 (1973).
[13]T. Kaneda, H. Matsumoto, and T. Yamaoka, J. Appl. Phys. **47**, 3135 (1976).
[14]J. D. Beck, C.-F. Wan, M. A. Kinch, and J. E. Robinson, Proc. SPIE **4454**, 188 (2001).
[15]J. D. Beck, C.-F. Wan, M. A. Kinch, J. E. Robinson, F. Ma, J. C. Campbell *et al.*, in *Proceedings of the IEEE LEOS Annual Meeting* (2003), Vol. 2, p. 849.
[16]A. R. J. Marshall, C. H. Tan, M. J. Steer, and J. P. R. David, Appl. Phys. Lett. **93**, 111107 (2008).
[17]A. R. J. Marshall, P. J. Ker, A. Krysa, J. P. R. David, and C. H. Tan, Opt. Express **19**, 23341 (2011).
[18]W. Sun, S. J. Maddox, S. R. Bank, and J. C. Campbell, in *72nd Device Research Conference* (2014), pp. 47–48.
[19]W. Sun, Z. Lu, X. Zheng, J. C. Campbell, S. J. Maddox, H. P. Nair, and S. R. Bank, IEEE J. Quantum Electron. **49**, 154 (2013).
[20]P. J. Ker, A. R. J. Marshall, A. B. Krysa, J. P. R. David, and C. H. Tan, in *17th Opto-Electronics and Communications Conference* (2012), pp. 220–221.
[21]R. Chin, N. Holonyak, G. E. Stillman, J. Y. Tang, and K. Hess, Electron. Lett. **16**, 467 (1980).
[22]F. Capasso, W. T. Tsang, A. L. Hutchinson, and G. F. Williams, Appl. Phys. Lett. **40**, 38 (1982).
[23]J. C. Campbell, S. Demiguel, F. Ma, A. Beck, X. Guo, S. Wang, X. Zheng, X. Li, J. D. Beck, M. A. Kinch *et al.*, IEEE J. Sel. Top. Quantum Electron. **10**, 777 (2004).
[24]P. Yuan, S. Wang, X. Sun, X. G. Zheng, A. L. Holmes, and J. C. Campbell, IEEE Photonics Technol. Lett. **12**, 1370 (2000).
[25]O.-H. Kwon, M. M. Hayat, S. Wang, J. C. Campbell, A. Holmes, Y. Pan, B. E. A. Saleh, and M. C. Teich, IEEE J. Quantum Electron. **39**, 1287 (2003).
[26]C. Groves, C. K. Chia, R. C. Tozer, J. P. R. David, and G. J. Rees, IEEE J. Quantum Electron. **41**, 70 (2005).
[27]S. Wang, R. Sidhu, X. G. Zheng, X. Li, X. Sun, A. L. Holmes, and J. C. Campbell, IEEE Photonics Technol. Lett. **13**, 1346 (2001).
[28]S. Wang, F. Ma, X. Li, R. Sidhu, X. Zheng, X. Sun, A. L. Holmes, and J. C. Campbell, IEEE J. Quantum Electron. **39**, 375 (2003).
[29]M. M. Hayat, O. Kwon, S. Wang, J. C. Campbell, B. E. A. Saleh, and M. C. Teich, IEEE Trans. Electron Devices **49**, 2114 (2002).
[30]S. Wang, J. B. Hurst, F. Ma, R. Sidhu, X. Sun, X. G. Zheng, A. L. Holmes, A. Huntington, L. A. Coldren, and J. C. Campbell, IEEE Photonics Technol. Lett. **14**, 1722 (2002).
[31]N. Duan, S. Wang, F. Ma, N. Li, J. C. Campbell, C. Wang, and L. A. Coldren, IEEE Photonics Technol. Lett. **17**, 1719 (2005).
[32]E. Yagyu, E. Ishimura, M. Nakaji, T. Aoyagi, K. Yoshiara, and Y. Tokuda, IEEE Photonics Technol. Lett. **18**, 1264 (2006).
[33]B. F. Levine, R. N. Sacks, J. Ko, M. Jazwiecki, J. A. Valdmanis, D. Gunther, and J. H. Meier, IEEE Photonics Technol. Lett. **18**, 1898 (2006).
[34]M. Nada, Y. Muramoto, H. Yokoyama, T. Ishibashi, and H. Matsuzaki, J. Lightwave Technol. **32**, 1543 (2014).
[35]J. P. Gordon, R. E. Nahory, M. A. Pollack, and J. M. Worlock, IEEE Electron Device Lett. **15**, 518 (1979).
[36]S. Rakshit and N. B. Charkraborti, Solid State Electron. **26**, 999 (1983).
[37]W. Clark, U.S. patent 6,747,296 (June 8, 2004).
[38]W. Sun, X. Zheng, Z. Lu, and J. C. Campbell, J. Quantum Electron. **48**, 528 (2012).
[39]M. S. Ferraro, W. Rabinovich, W. Clark, W. Waters, J. C. Campbell, R. Mahon, K. Vaccaro, B. Krejca, and P. D'Ambrosio, Opt. Eng. **55**, 111609 (2016).
[40]M. E. Woodson, M. Ren, S. J. Maddox, Y. Chen, S. R. Bank, and J. C. Campbell, Appl. Phys. Lett. **108**, 081102 (2016).
[41]M. Ren, S. J. Maddox, M. E. Woodson, Y. Chen, S. R. Bank, and J. C. Campbell, Appl. Phys. Lett. **108**, 191108 (2016).
[42]I. Watanabe, M. Tsuji, K. Makita, and K. Taguchi, IEEE Photonics Technol. Lett. **8**, 827 (1996).
[43]L. G. Vaughn, L. R. Dawson, H. Xu, Y. Jliang, and L. F. Lester, "Characterization of AlInAsSb and AlGaInAsSb MBE-grown digital alloys," in *Symposium M – Progress in Semiconductors II–Electronic and Optoelectronic Applications* (Mat. Res. Soc. Symp. Proc., 2002), Vol. 744, pp. M7.2.1–M7.2.12.
[44]L. G. Vaughn, in *Physics and Simulation of Optoelectronic Devices XIII* (SPIE, 2005), p. 307.
[45]L. G. Vaughn, Ph.D. dissertation, The University of New Mexico, 2006.
[46]S. A. Plimmer, J. P. R. David, D. C. Herbert, T.-W. Lee, G. J. Rees, P. A. Houston, R. Grey, P. N. Robson, A. W. Higgs, and D. R. Wright, IEEE Trans. Electron Devices **43**, 1066 (1996).
[47]Y. L. Goh, J. S. Ng, C. H. Tan, W. J. Ng, and J. P. R. David, IEEE Photonics Technol. Lett. **17**, 2412 (2005).
[48]C. Lenox, P. Yuan, H. Nie, O. Baklenov, C. Hansing, J. C. Campbell, A. L. Holmes, Jr., and B. G. Streetman, Appl. Phys. Lett. **73**, 783 (1998).
[49]F. Capasso, W. T. Tsang, and G. F. Williams, IEEE Trans. Electron Devices **30**, 381 (1983).
[50]M. Ren, S. J. Maddox, Y. Chen, M. E. Woodson, J. C. Campbell, and S. R. Bank, Appl. Phys. Lett. **108**, 081101 (2016).
[51]L. Esaki and R. Tsu, IBM J. Res. Dev. **14**, 61 (1970).
[52]S. L. Chuang, in *Physics of Optoelectronic Devices*, edited by J. W. Goodman (Wiley, 1995), p. 605.
[53]S. J. Maddox, S. D. March, and S. R. Bank, J. Cryst. Growth Des. **16**, 3582 (2016).
[54]I. Vurgraftman, J. R. Meyer, and L. R. Ram-Mohan, J. Appl. Phys. **89**, 5815 (2001).
[55]R. de L. Kronig and W. G. Penney, Proc. R. Soc. London, A **130**, 499 (1931).